Proportional-Resonant Controller And LCL Filter Design For Single-Phase Grid-Connected PV Micro-Inverters

P. Cossoli, M. Cáceres, L. Vera, A. Firman, A. Busso
Grupo en Energías Renovables (GER)
Universidad Nacional del Nordeste, UNNE
Av. Libertad 5470 – 3400 Corrientes. Argentina.
pcossoli@ger-unne.com.ar

***Abstract*—This paper presents a brief behavior description of LCL filters through the analysis of its frequency response and the convenience of its use instead L filters. Moreover, the equations that allow its design and implementation are also described. Regarding the Proportional Resonant (PR) controllers, their behavior, discretization techniques and digital implementation are also studies. The developed systems are evaluated by mathematical model simulation and experimental prototype test. It is concluded that, for inverters operating as a current source, the PR controllers are suitable to follow a sinusoidal reference signal. On the other hand, LCL-type filter largely eliminates the harmonic content of the output current, making it compatible for Grid-Connected PV micro-inverters.**

Keywords—solar energy; grid-connected inverter; proportional resonant controller

I. INTRODUCTION

The growing worldwide energy demand along with trends to reduce fossil resources exploiting has driven renewable energy sources development. Among them, solar energy photovoltaic conversion technology (PV) had a high grade of development in last decades [1].

In Grid-Connected PV Systems all generated energy must be injected into a utility grid by an inverter, whose function is to adapt and transfer PV power. Pulse-Width-Modulation (PWM) techniques are commonly used to control frequency and phase of injected current into a grid, however, generate unwanted harmonics. Therefore, the output filter of the inverter fulfills fundamental function in harmonics suppression. The LCL filter topology is generally preferred instead L or LC filters because of it great harmonics suppression capability. Nevertheless, the LCL filter presents a resonant peak that affects the system stability and control scheme design of grid-connected inverter must take that behavior into consideration [2].

According to IEC 61727 Standard [3], the total harmonic distortion (THD) of current injected into the grid must be within the limits. Proportional Integral (PI) controllers are commonly used in current sources inverters; however this solution has drawbacks: unable to track sinusoidal signals with zero steady-state error and a low disturbance rejection capability. On the other hand, a Proportional Resonant (PR) controller presents an infinite gain at the selected resonant frequency; therefore, zero steady-state error can be achieved [4].

This paper presents the design and implementation of a LCL filter and a comparison with other filters commonly used in grid-connected PV micro-inverters. The design of PR controllers and digital implementations are studied. The performance of the complete system is evaluated through simulations and experimental prototype test. This prototype is the first grid-connected PV micro-inverter carried out in the North of Argentina.

II. GRID-CONNECTED PV MICRO-INVERTER OVERVIEW

Figure 1 shows the typical topology of a two-stage grid-connected PV micro-inverter. The boost DC-DC converter step up the voltage of the PV module to a suitable level for next stage. The DC-AC inverter, normally composed by an H-bridge, produces a proper sinusoidal current compatible with the grid. The LCL output filter attenuates harmonics generated from the inverter output and a digital controller ensures unit-power-factor operation.

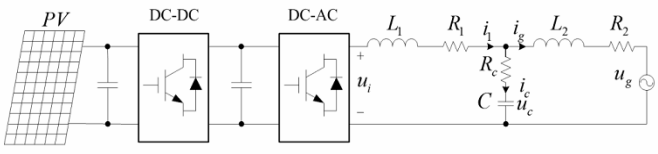

Fig. 1. Two-stage grid-tie PV system with LCL filter typical topology

III. OUTPUT FILTER ANALYSIS

The output filter is essentially an impedance adapter, making it possible to connect the inverter output to a grid and filtering the harmonic content produced by the modulation technique.

978-1-5386-5844-4/18/$31.00 ©2018 IEEE

A. *Frequency response*

According to Fig. 1 the Laplace transfer function of the LCL filter is given by (1) in term of grid current and inverter output voltage [5].

$$H_{LCL}(s) = \frac{i_g}{u_i} = \frac{1}{L_1 C L_2 s^3 + (L_1 + L_2)s} \tag{1}$$

Where, L_1 and L_2 are the inverter-side and grid-side output inductor, respectively. The internal resistances, R_1 and R_2 are neglected. In order to avoid stability problems a Damping Resistance (DR) can be added in series with capacitor C to mitigate resonance peak, (2) represents this case.

$$H_{LCL\_DR}(s) = \frac{CR_c s + 1}{L_1 C L_2 s^3 + C(L_1 + L_2)R_c s^2 + (L_1 + L_2)s} \tag{2}$$

Figure 2 compares the Bode diagram of (1) and (2). Frequency response of an L filter is showed too. At low frequency LCL and L filters has a similar dynamic response. In high frequency range, LCL filter presents a higher attenuation than the L filter. The main drawback of LCL filters without a DR is the resonance peak at resonant frequency. The DR reduces that peak, but at higher frequencies presents less attenuation and generates power losses.

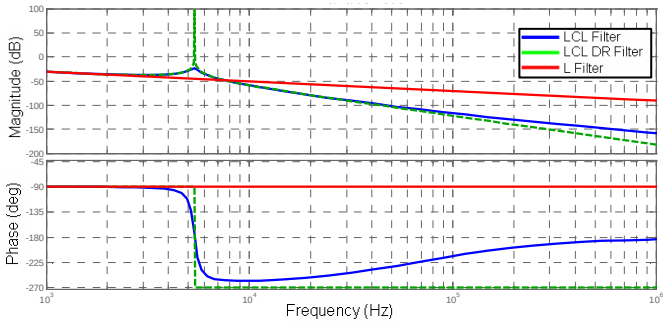

Fig. 2. LCL and L filters Bode diagrams.

B. *Systematic filter design*

This section presents general considerations for LCL filters design. A more detailed analysis can be found in [6]. The following parameters must be defined: RMS voltage inverter output (E_n), rated active power (P_n), DC-Link voltage (V_{DC}), grid frequency (f_g) and switching frequency (f_{sw}).

The base impedance is given by (3) and can be interpreted as the output impedance that the inverter sees. In the same way (4) defines the base capacitance.

$$Z_b = \frac{E_n^2}{P_n} \tag{3}$$

$$C_b = \frac{1}{\omega_g Z_b} \tag{4}$$

For filter capacitance C, as general rule, the maximum power factor variation seen by the grid must not exceed 5%, thus:

$$C = 0{,}05 C_b \tag{5}$$

The inverter-side inductor L_1 can be calculated by (6). Where, ΔI_{Lmax} is the maximum current ripple at the output of DC/AC inverter. A conservative value for this parameter can be 20% of the rated output current.

$$L_1 = \frac{V_{DC}}{6 f_{sw} \Delta I_{L\max}} \tag{6}$$

The grid-side inductor is determined taking into account the desired harmonic attenuation. Then, the value of L_2 is expressed as a proportion of L_1.

$$L_2 = r L_1 \tag{7}$$

Finally, all filter components should verify that the resonance frequency is within a range given by (8).

$$\omega_{resonancia} = \sqrt{\frac{L_1 + L_2}{L_1 L_2 C}}$$
$$10 f_g < f_{resonancia} < 0{,}5 f_{sw} \tag{8}$$

IV. CONTROL SCHEME

The control scheme of a micro-inverter is composed of several sub-systems that interact with each other. The MPPT algorithm is responsible for polarizing the PV module at its maximum power point. Furthermore, a PLL algorithm guarantees unitary power factor. Papers in the literature present different MPPT [7] and PLL algorithms [8].

On the other hand, sinusoidal current reference demands special controller topology. The classic PI controller has a quick step response and zero steady-state error, but is unable to track sinusoidal reference signals. Instead, the PR controller has an infinite gain at the resonant frequency and eliminates steady-state error at that frequency [9].

A. *PR Controller Frequency Response*

The Laplace transfer function of an ideal PR controller is given by (9).

$$H_{PR}(s) = K_p + \frac{2K_r s}{s^2 + \omega_0^2} \tag{9}$$

Where K_p is the proportional gain, ω_0 is the resonance frequency and K_r is the gain at ω_0. Figure 3 shows the Bode diagram for (9).

To avoid stability problems associated with an infinite gain, the non-ideal PR controller given by (10) is preferred instead (9).

$$H_{PR}(s) = K_p + \frac{2K_r \omega_{PRc} s}{s^2 + 2\omega_{PRc} s + \omega_0^2} \tag{10}$$

Where, ω_{PRc} controls the bandwidth around the resonance frequency. The aim of this improvement is reduce the influence of the grid fundamental frequency variation.

Figure 4 shows the Bode diagram of the non-ideal PR controller with a parametric variation of K_p and K_r. The K_p term mainly determines the controller dynamics, while K_r determines the amplitude of the gain at a selected resonance frequency.

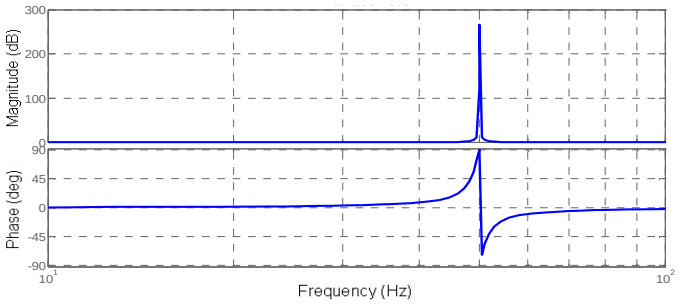

Fig. 3. Bode diagram of an ideal PR controller

B. *Digital Implementation*

The transfer function given in (9) is in the continuous time-domain and must be converted to discrete time-domain for digital implementation (microcontroller or micro processor).

The resonant term of (9) is also referred as second order generalized integrator.

$$R(s) = \frac{s}{s^2 + \omega_0^2} \tag{11}$$

A method to implement (11) in the discrete time-domain consists in discretizing the continuous transfer function by one of the techniques proposed in [10]. The most commonly used technique is the Tustin with frequency prewarping. The result of applying this technique to (11) is show in (12).

$$R_{tp}(z) = \frac{\sin(\omega_0 T_s)}{2\omega_0} \frac{1 - z^{-2}}{1 - 2z^{-1}\cos(\omega_0 T_s) + z^{-2}} \tag{12}$$

It is important to be aware that discretization process itself produces displacements in the original location of poles and zeros. Furthermore, this effect will depend on the discretization technique used. This study is beyond the scope of this paper, but a detailed analysis can be found in [11].

Finally, (13) shows the difference equation form of the second order generalized integrator. This equation allows to carry out an algorithm that implements the PR controller.

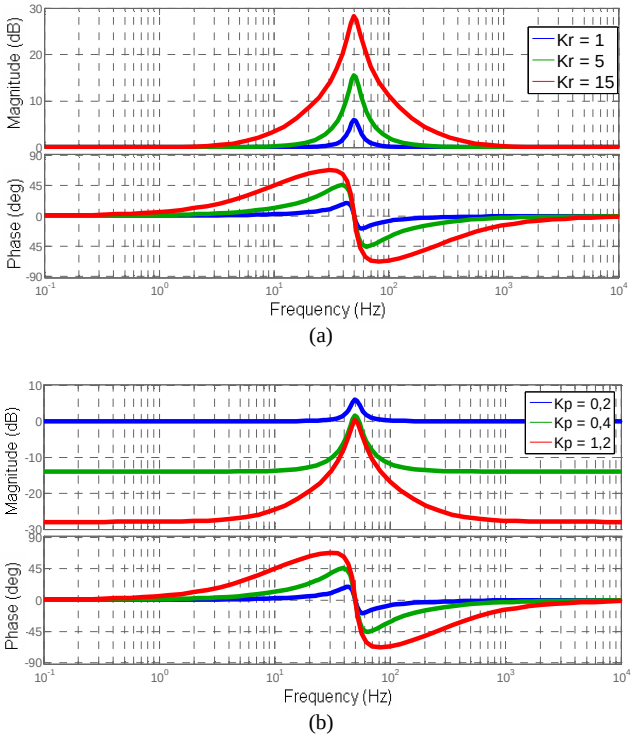

Fig. 4. Bode diagram of a non-ideal PR controller. (a) $K_p = 1$; (b) $K_r = 1$.

$$u_r(k) = k_r[e(k-1) - e(k-2)] - a_r u(k-1) - u(k-2) \tag{13}$$

Where a_r is given by (14) and T_s is the sampling period.

$$a_r = 2\cos(\omega_0 T_s) \tag{14}$$

V. System Setup

Table I shows the parameters for LCL filter design and Table II lists the values obtained for the filter components using the equations described in Section IV.

TABLE I. DESIGN PARAMETERS FOR LCL FILTER

Symbol	Parameter	Value
E_n	RMS voltage inverter output	220 V
P_n	Rated active power	400 W
V_{DC}	DC-Link voltage	450 V
f_g	Grid frequency	50 Hz
f_{sw}	Switching frequency	28 kHz

TABLE II. LCL FILTER. COMPONENT VALUES

Symbol	Parameter	Value
L_1	Inverter-side inductor	1.2 mH
L_2	Grid-side inductor	860 µH
C	Filter capacitor	1.2 µF
$f_{resonancia}$	Resonance frequency	6.5 kHz

The PR controller was designed using MATLAB and discretized using the Tustin method with frequency prewarping. The controller parameters are shown in Table III.

TABLE III. PARAMETERS OF THE PR CONTROLLER

Symbol	Parameter	Value
K_p	Proportional gain	0.2
K_r	Resonant gain	10
ω_c	Bandwidth	6
T_s	Sampling period	81.25 µs

A. *Mathematical model simulation*

Simulation model was carried out using PSIM. Figure 5 show a full bridge topology with four MOSFET. The designed LCL filter is presented with internal resistance for each inductor and the damping resistance for capacitor *C*. The grid was modeled by constant voltage source and grid impedance.

The switching scheme consists of sinusoidal PWM (SPWM) modulation with unipolar voltage switching. The algorithm of PR controller was implemented in a block of C code. Both blocks are omitted in Fig. 5. The grid was modeled through an ideal AC source in series with impedance Z_g. No isolation transformer was used in simulation scheme.

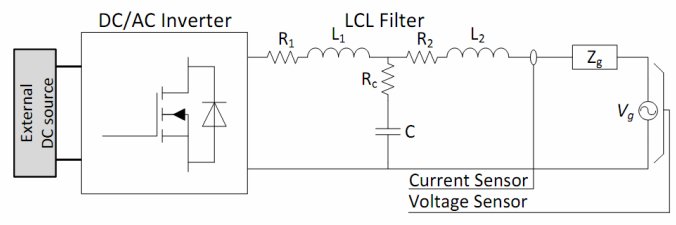

Fig. 5. Simulation scheme

B. *Experimental prototype*

For design validation of the LCL filter and PR controller, a first micro-inverter prototype was made (Fig. 6).

The control strategy and PLL algorithm was implemented in 32-bits, floating point microcontroller TM4C123GH from Texas Instrument. Moreover, the SPWM modulation was generated analogically and the injected current is measured through a Hall-effect sensor.

On the other hand, the coupling with the grid was carried out through an isolation transformer (not shown in Fig. 6).

The experimental measurement of grid voltage and current was made using a Fluke differential oscilloscope, model 190-104, on the isolation transformer primary-side. Also, the data was acquired with the same equipment and analyzed through MATLAB.

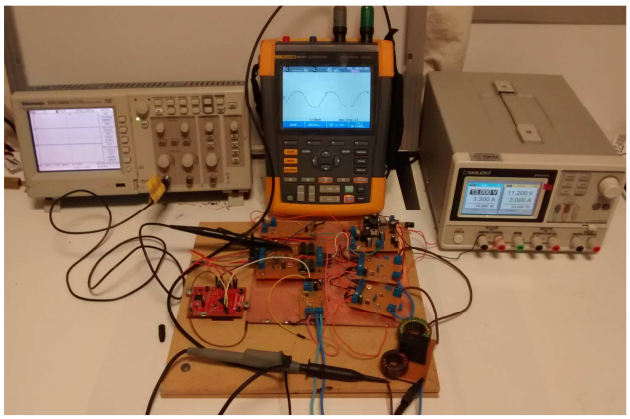

Fig. 6. Laboratory scale prototype.

The system performance was evaluated taking into account the controller capability to track a sinusoidal reference signal and the phase error produced. Furthermore, the amplitude of the more relevant harmonics and the THD of the injected current was analyzed and compared with the IEC 61727 standard limits. The evaluations were carried out in both mathematical simulation model and experimental prototype.

VI. SIMULATION AND EXPERIMENTAL RESULTS

Figure 7 shows reference and grid injected current signals obtained through simulations. The reference current was set at 1.8 A RMS. It can be observed that the harmonic content is low and the THD of the injected current is lower than 3%. The power factor obtained was equal to 0.99.

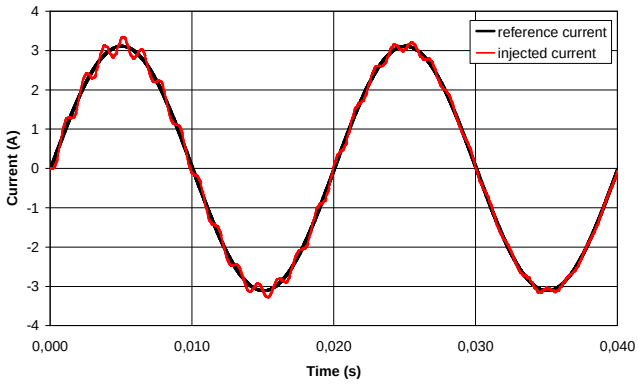

Fig. 7. Simulation results. Reference current and injected current to the grid.

In the experimental prototype reference current was set at same value (1.8 A). Figure 8 shows experimental waveforms of grid voltage and injected current. As can be seen, there is no phase error noted between grid current and voltage. The power factor obtained was equal to 0.98.

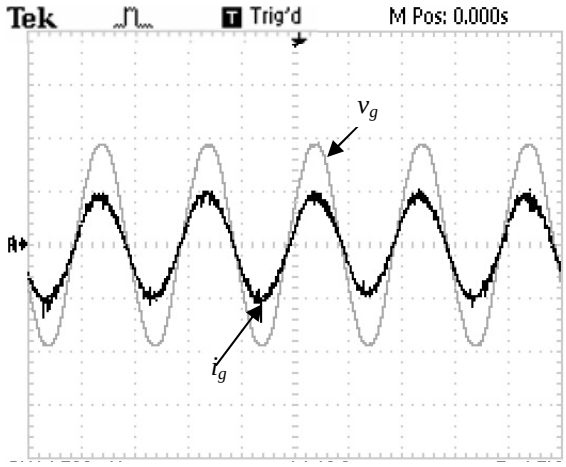

Fig. 8. Experimental results. Grid voltage (vg). Injected current into the grid (ig).

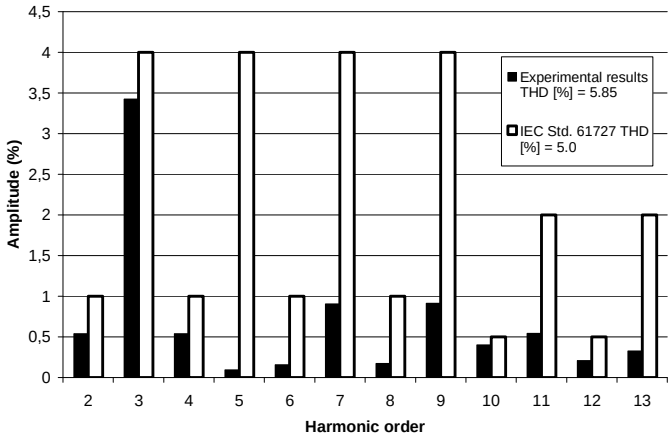

Fig. 9. Experimental results. Harmonic components of the injected current and limits for IEC 61727 Std.

Figure 9 shows the harmonic components of the injected current and the IEC 61727 standard limits for reference. The even harmonics, 2nd and 4th, exhibit a value of 0.5%. This is due imperfections in the modulation scheme.

On the other hand, the 3rd harmonic has a value of 3.4%, and its amplitude is mainly due to the influence of the isolation transformer. It is considered that implementing a selective PR controller centered in the 3rd harmonic can further reduce his amplitude. Although the harmonic content meets the IEC 61727 standard limits; the THD was 5.85%, slightly above the maximum allowed.

VII. Conclusions

This paper presents basic concepts about LCL filter and PR controller. A simple and structured method for a PV micro-inverter LCL filter and PR controller design has been described. The performance of the complete system is evaluated through simulations and experimental prototype test.

The results shows that LCL filters are suitable for mitigate higher order harmonics. In addition, the design approach is also applying to low power grid-connected PV systems such as micro-inverters.

As it was shown, the gain of PR controllers becomes infinite on the resonance frequency. This makes that the PR controller can track a sinusoidal reference signal with zero steady-state error. On the other hand, discretization techniques of the controller allow a simple implementation and a modest calculation requirement. Furthermore, the THD of the injected current can be improved adding selective PR controllers. And this can be carried out in future works using the same prototype designed.

Finally, it was found that the THD of the injected current is slightly higher than the IEC 61727 standard limits. However, it is the first prototype designed in Northern Argentina. Therefore, the authors consider that the results obtained are satisfactory.

References

[1] Trends 2016 in Photovoltaic Applications (2016). International Energy Agency (IEA), Photovoltaic Power Systems Programme (PVPS).

[2] Teodorescu, R., Blaabjerg, F., Borup, U., & Liserre, M. (2004). A new control structure for grid-connected LCL PV inverters with zero steady-state error and selective harmonic compensation. In Applied Power Electronics Conference and Exposition, 2004. APEC'04. Nineteenth Annual IEEE (Vol. 1, pp. 580-586). IEEE.

[3] IEC Standard Photovoltaic (PV) systems – characteristics of the utility interface, IEC Std. 61727, 2009.

[4] Zmood, D. N., & Holmes, D. G. (2003). Stationary frame current regulation of PWM inverters with zero steady-state error. IEEE Transactions on power electronics, 18(3), 814-822.

[5] Reznik, A., Simoes, M. G., Al-Durra, A., & Muyeen, S. M. (2014). LCL filter design and performance analysis for grid-interconnected systems. IEEE Transactions on Industry Applications, 50(2), 1225-1232.

[6] Liserre, M., Blaabjerg, F., & Hansen, S. (2005). Design and control of an LCL-filter-based three-phase active rectifier. IEEE Transactions on industry applications, 41(5), 1281-1291.

[7] Esram, T., & Chapman, P. L. (2007). Comparison of photovoltaic array maximum power point tracking techniques. IEEE Transactions on energy conversion, 22(2), 439-449.

[8] Ciobotaru, M., Teodorescu, R., & Blaabjerg, F. (2006, June). A new single-phase PLL structure based on second order generalized integrator. In Power Electronics Specialists Conference (pp. 1-6).

[9] Teodorescu, R., Blaabjerg, F., Liserre, M., & Loh, P. C. (2006). Proportional-resonant controllers and filters for grid-connected voltage-source converters. IEE Proceedings-Electric Power Applications, 153(5), 750-762.

[10] Rodriguez, F. J., Bueno, E., Aredes, M., Rolim, L. G. B., Neves, F. A., & Cavalcanti, M. C. (2008, November). Discrete-time implementation of second order generalized integrators for grid converters. In Industrial Electronics, 2008. IECON 2008. 34th Annual Conference of IEEE (pp. 176-181). IEEE.

[11] Yepes, A. G., Freijedo, F. D., Doval-Gandoy, J., Lopez, O., Malvar, J., & Fernandez-Comesana, P. (2010). Effects of discretization methods on the performance of resonant controllers. IEEE Transactions on Power Electronics, 25(7), 1692-1712.